



A Software Prototype for Treatment Planning and Intervention Support of Robot-Assisted Radiofrequency Ablations of Vertebral Metastases

Nico Merten¹, Sylvia Saalfeld¹, Magnus Hanses², Mathias Becker³,
Simon Adler², Bernhard Preim¹

¹ Otto-von-Guericke University, Department of Simulation and Graphics

² Fraunhofer Institute for Factory Operation and Automation (IFF)

³ University Hospital Magdeburg, Institute of Neuroradiology

To cite this version:

Merten, N., Saalfeld, S., Hanses, M., Becker, M., Adler, S., Preim, B. A Software Prototype for Treatment Planning and Intervention Support of Robot-Assisted Radiofrequency Ablations of Vertebral Metastases . *16. Jahrestagung der Deutschen Gesellschaft für Computer- und Roboterassistierte Chirurgie (CURAC)*. Pages: 89–94. Hanover, Germany. 2017.

Abstract

When physicians want to treat vertebral body metastasis with radiofrequency ablations they have to consider many patient-specific factors, such as the metastasis count and their localization. There is a high interest in robotic-assisted approaches for this type of therapy, because they are hard to plan and execute. In this paper, we present our software prototype to support the planning and intervention execution stages of this therapy. Our work provides a list of nine application requirements, which we derived from interviewing our clinical and technical colleagues. Those requirements, while being tailored to a given setup, are constructed as general as possible to be reusable for different configurations. We focused on three intervention stages, namely image exploration, therapy planning, and intervention execution and mapped them to a systematic application usage design. From there, we combine multiple image and direct volume renderers with superimposed risk structure segmentations and applicator geometry. As a result, we designed a prototype to fulfill our requirements including a discussion of required visualizations and functionalities.

1 Problem

If a vertebral body is afflicted with metastatic cancer, it can weaken the stability of the spine, which can result in pain, neurologic dysfunction, and fractures [Schaefer et al., 2003]. To approach this problem, image-guided radiofrequency ablations (RFAs) can be used. When they are used as an additional therapy, they are commonly combined with chemo- and radiation therapies [Gazis et al., 2014] and their implementation depends on patient-specific factors, such as the overall tumor load, metastasis count, their distribution and localization. Depending on the part of the spine where the afflicted vertebra is located, surgical instruments are inserted from dorsal or lateral direction. For the more common dorsal direction, trocars or drills are used to create pathways for the RFA needles into the vertebra. Although this procedure requires a certain force to penetrate the vertebra, care and precision are also very important to preserve risk structures near or inside a targeted vertebra, such as the neuroforamina or spinal cord. Additionally to this physical stress and radiation exposure by the imaging system and ablation needles, therapy-specific risks of RFAs can range from immense pain from comminuted vertebral bodies to paraplegia or death.

To reduce these problems, physicians can use an assistant robot for RFA interventions. In [Hanses et al., 2016], Hanses et al. presented a basic robotic assistance system using a KUKA LBR robotic arm [Bischoff et al., 2010] (see Fig. 1). This system uses a hand-guiding approach, where the robot augments the physician’s abilities to perform tremor-free, scaled and constrained motions. This approach is a special case of human-robot collaboration, because parts of the process involve inserting instruments into a human body. Therefore, the robotic arm’s use has to be safe, so that it does harm neither the medical staff, nor the patient. To ensure this, a clear and intuitive human-robot interface is mandatory: It has to provide all the information needed by the physician to safely perform the RFA with robotic assistance. This includes, but is not limited to, intervention planning steps, sensor data, and movement constraints of the robotic arm. With all these information at hand, the physician can make sophisticated assessments during the intervention, thus, the risks of incorrect use can be reduced.

2 Materials and Methods

Given our clinical context and technical setup, we aimed to extend a basic human-robot interface with a software prototype that focuses on visualizations to support the physician. Visualizable information include image data sets, hardware states of the robotic arm, its trajectory, and measured or computed attributes like the Bone Mineral Density (BMD) [Schreiber et al., 2014]. The latter can be done to predict the change in forces during needle insertion on the intensity gradient of the image data, but for now we



Figure 1: The basic model of the KUKA LBR robotic arm [Bischoff et al., 2010]. For surgical support, a holder can be mounted to the tip of the robot that can carry surgery tools, such as a drill. During the intervention, the physician and robotic arm cooperatively insert these tools into the patient.

used the unaltered Hounsfield Units (HUs) of the input image. We interviewed our clinical partners and derived the following list of application requirements for our prototype:

- [R1] It should be possible to segment risk structures in the prototype. Possible risk structures include the spinal canal, neuroforamina, intercostal nerves, and aorta.
- [R2] It should be possible to place and orientate an applicator for surgical instruments in the prototype. An example is a drill to create an access path to a metastasis with robotic assistance.
- [R3] Depending on the metastases' sizes and distribution, a single RFA needle may not be sufficient for a complete ablation. Therefore, the user should be able to place and orientate two applicators.
- [R4] Medical image scans should be presented in 2D and Direct Volume Rendering (DVR) views.
- [R5] When the image data is rendered, it should be possible to superimpose them with 2D and 3D representations of the applicators and segmentations.
- [R6] The robot has three different operation modes: Approach the point of insertion, collaborative insertion between physician and robotic arm, and holding the final position. The prototype has to show which mode the robotic arm is in at any time.
- [R7] The prototype has to consider two types of safety margins:
 - Around the robotic arm's periphery inside the operating room.
 - Around the segmented risk structures in the 2D and 3D views.The prototype should show whether persons are tangent to the robotic arm's safety margin and if operation instruments are tangent to segmented risk structures.
- [R8] The prototype should visualize the HUs along the applicators' paths, which implicitly show the resistance the operating surgeon can expect when he inserts instruments into the patient's body.



Figure 2: In the Import tab, a data set can be imported and displayed in 2D and 3D. An adjustable transfer function can be applied to all views with the APPLY LUT button. At the bottom right, two status displays indicate whether our prototype has a connection to the MEVIS SAFIR or the CAScination system. This was important because our project partners want to use our prototype as an easy-to-customize, visualization-heavy interface between these systems. Darkened buttons and status symbols indicate that the respectively associated functionalities are deactivated.

[R9] In the future, the robot will be able to perform a respiratory correction. For this, the patient’s respiratory movement has to be tracked. During the intervention, the actual instrument’s trajectory has to be visualized in relation to its final position, which was defined during intervention planning.

We divided these requirements in three groups with respect to the three robotic arm’s modes that Hanses et al. describe in [Hanses et al., 2016], namely Data Import ([R4]), Planning ([R1-R3], [R5], [R7-R8]), and Intervention ([R6], [R9]). From now on, when we describe the implementation of a certain requirement, we use the Notation [R*], analog to citations, where * will be substituted with the corresponding numbering from the list above.

We implemented our prototype in MeVisLab 2.8.2 [Ritter et al., 2011]. For now, we only used a single CT data set of a scanned upper body phantom.

3 Results

In the first Graphical User Interface (GUI) tab, namely Data Import, the user can import and explore medical image data sets [R4]. Figure 2 shows this tab’s contents. Here, the user imported the CT phantom data set.

Below the import area, the GUI is divided into two parts, which contain 2D and 3D views. Additionally, the user can use a transfer function panel to map the HUs to colors and opacities. This functionality can be toggled on or off by pressing a button. Our project partners want to use our

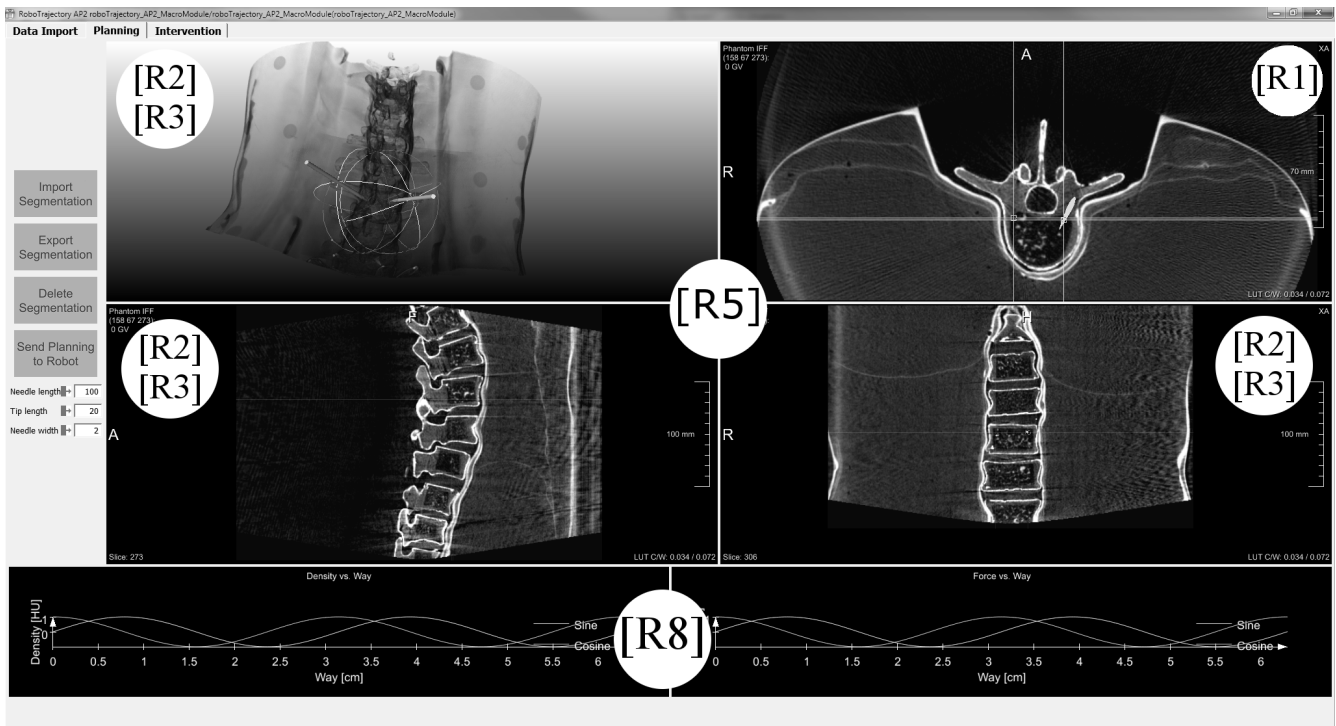


Figure 3: In the Planning tab the user can explore the imported image data in four linked 2D and 3D views. Here, he can segment risk structures and interact with two needle applicators. He can use the buttons on the left side to import, export and delete segmentations. Furthermore, the applicators' length, width, and tip length can be altered. Two graphs at the bottom show the HUs and expected forces for each applicator needle along their planned trajectories from the 2D views above.

prototype as an easy-to-customize, visualization-heavy software interface between the Software Assistant for Interventional Radiology (MEVIS SAFIR, Fraunhofer MEVIS, Bremen, Germany) and Computer Assisted Liver Surgery and Interventions Software (CAsCination, CAsCination AG, Bern, Switzerland). In their workflow, MEVIS SAFIR [Weihsen et al., 2006] will be used to segment and export risk structures. The CAsCination system [Peterhans et al., 2010] will be used to optically track the surgical instruments, which are mounted on the robotic arm's tip. Therefore, two status symbols at the bottom indicate whether the connections to these systems are active.

On the left side in the Planning tab are buttons to import, export or delete segmentations and to manipulate features of the applicator needles, such as their length and width (see Fig. 3). The main part focuses on four linked 2D and 3D views: The user can place two applicators in the 2D views [R2, R3] and segment risk structures [R1], whereas the applicator's orientation can be adjusted in the 3D views [R2, R3]. Here, linking refers to the linking of views: If any segmentation or applicator is altered in one view, the change is visible in all other views, too. Additionally, the images are superimposed with less opaque rendered and colored geometries [R5].

At the bottom of Figure 3 are two graphs. In the left graph, the HUs (y-axis) are plotted along the applicators' paths (x-axis). The result visualizes the change of radio densities: Upward slopes indicate transitions from softer to harder structures and downward slopes show the opposite. The HUs could then be converted to force values. When these force values would then be visualized, the resulting graph plot would present an estimation of how much force the robot's operator would have to use when he moves the mounted instrument along one of these planned trajectories. The graph plot could also be interpreted in

a different way, because it also shows how much resistance the operator can expect along an instrument’s trajectory [R8]. We did not implement the described functionality yet and refer to our discussion in the following section.

We also used multiple 2D and 3D views in the Planning Tab. Additionally to the segmentations and applicators from the Intervention tab, the images are further superimposed by new applicators. They represent the positions and orientations of the tracked instruments (see Fig. 4). We wanted the user to perceive the planned trajectories as a visual frame of reference, because during an actual intervention his or her visual focus should be on the tracked information. To do that, while using the exact same color for each pair of applicators, the planned trajectories are rendered less opaque and the tracked trajectories are rendered fully opaque. Finally, when this information superimpose the relatively dark CT images, the applicators that represent the tracked instruments appear much brighter, thus the user will focus on them.

At the bottom, several buttons indicate robot’s current mode [R6] and other states:

- Approach the point of insertion: The robot moves towards the patient’s body.
- Switch on the tactile floor pressed/ not pressed: The physician and robotic arm can only move cooperatively, if this switch is pressed.
- Final position reached: The robot reached the planned target position in cooperative guidance and holds it.
- Breathing correction: The robot performs movements for respiratory correction.
- Risk structures: A tool is tangent to a segmented risk structure or intersects it [R7].
- Periphery: Objects or persons in the operating room are too close to the robot [R7].

4 Discussion

In the last two sections, we introduced a list of nine requirements and their implementations. In this section, we want to discuss shortcomings of our prototype and how we will address them in our future work.

Our clinical colleagues record multiple, multimodal medical image scans prior to the intervention. These scans include CT-, MRI T1- (before and after contrast agent administration), MRI T2-, and MRI Short Tau Inversion Recovery Sequence (STIR) recordings. In its current state, our prototype can only process one single scan, but if the use of multimodal scans can be motivated clinically, our community could do research on new methods and algorithms that could benefit the planning and execution of RFAs. For example, although CT scans exceed in depicting bony structures, the origin or distribution of metastases cannot be assessed in these scans. Therefore, a combination with an MRI scan may be beneficial.

We did not implement requirement [R7] yet. For the first part, the robot’s periphery will be checked to be free of obstacles, such as medical staff or imaging devices. To do that we could use a camera’s image stream, but, for now, we did not work on this aspect. For the second part, we first have to create the segmentation’s safety margins and then check if the planned applicator’s trajectories are tangent to them or if there are any intersections. This test could either be carried out automatically or by pushing a button, whereby the real-time capability for the first approach strongly depends on the number of segmentations. It is also necessary to consider how the prototype

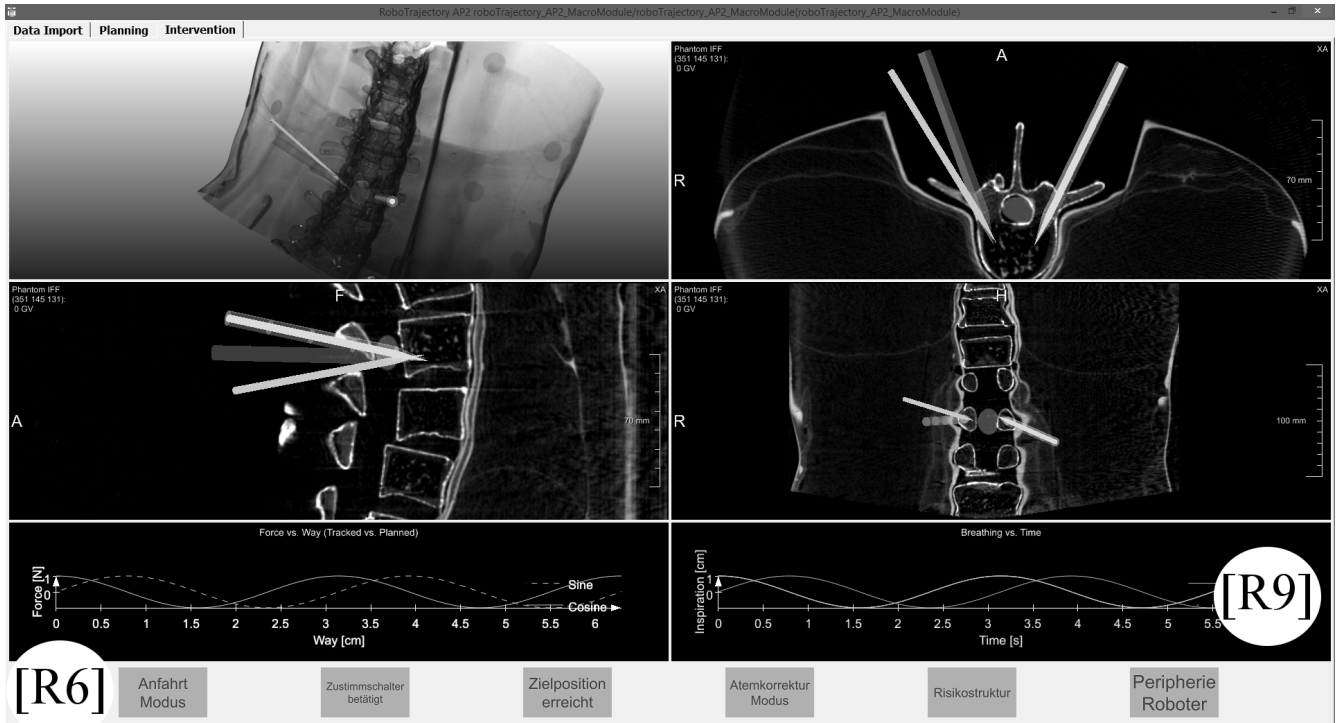


Figure 4: The segmented risk structures and planned trajectories are transferred from the Planning to the Intervention tab. In addition, the tracked positions and orientations of the mounted instruments are added. When the medical images are superimposed, the planned trajectories are rendered less opaque, while the tracked trajectories are rendered fully opaque. Our technical colleagues plan to mount a manometer to the robot. Therefore, the left graph could be used to present the estimated and measured force values. Additionally, when the system will be able to track the patient's respiratory movement, the right graph plot could depict this movement over time. At the bottom, several status symbols indicate the robot's current mode.

communicates problematic scenarios to the user: It could be possible to open a new window where the problematic pairs of segmentations and applicators are presented to the user. If the user wishes to see all segmentations and applicators, the problematic pairs could be highlighted by rendering them fully opaque while reducing the opacity for everything else. Another approach could be to offer a series of alternative applicator placements and orientations, which do not exhibit problematic pairs.

Our technical colleagues plan to mount a manometer on the robot. The manometer will measure the occurring forces the drill has to work against as it is inserted into the patient. Therefore, we worked on a draft where the pre-calculated and intra-operationally measured force values are combined in one graph (see [R8] and Fig. 3). With that, the robot's operator would have an additional visualization to examine if the instrument is approximately moved along its planned trajectory. In theory, if the graph line that represents the intra-operationally measured force values deviates too much, the drill could be moved along an unplanned and maybe strongly undesired path.

Another task of our future work is the implementation of requirement [R9]. The main challenge is that the physicians define the instrument's final destination in pre-operatively recorded image scans, which are static, but during the intervention, the patient's respiratory movement constantly displaces position. This displacement can range to 8 cm or more, depending on the patient's physique and in which part of his or her body the intervention will be implemented. For this, we drafted another graph plot, where the user can examine the instrument's planned destination and its intra-operatively tracked position with respect to the patient's respiratory movement.

One possibility to implement the requirements [R8] and [R9] is via graph plot visualizations. The main challenge is to present all information to the user, so that he or she can interpret the result easily, while not being distracted. This is even more important, because the resulting graph plots could be seen during the intervention, where the physician's focus should stay on the used instruments and the patient. In our scenario, the most complicated case is to visualize four lines in one graph, where the estimated and measured force values are presented for two surgical instruments. For this, we want to try to adapt the line halos from Everts et al. [Everts et al., 2009]: To perceive the estimated force values, which were calculated during the intervention planning, in the visual background, white halos are added to the graph line which depicts the measured force values during the intervention. As a result, the first graph line is presented discontinuously, thus it will be perceived as a visual frame of reference for the second graph line. Different approaches include adapting the lines' thickness, their transparencies, or the use of color.

Finally, we did neither carry out a detailed evaluation with our colleagues nor independent domain experts, because we did not implement the requirements [R7-R9] yet. Furthermore, whereas using a CT-scanned upper body phantom sufficed for our prototype, we will have to test our methods with real datasets in the near future.

5 Conclusion

In this work, we presented our visualization-focused software prototype to support robotic assisted Radiofrequency Ablations in the spine. We presented a list of requirements we extracted from interviews with clinical and technical experts, which are tailored to their given setup, while being constructed as general as possible. These requirements were divided into three groups and we implemented those using a dedicated visualization for every requirement. Additionally, when no straightforward implementation was possible, we presented ideas and concepts that are the base for our currently ongoing and future work.

Acknowledgement

The work of this paper is partly funded by the Federal Ministry of Education and Research within the Forschungscampus *STIMULATE* under the grant numbers 13GW0095A and 13GW0095B.

References

- [Bischoff et al., 2010] Bischoff, R., Kurth, J., Schreiber, G., Koeppe, R., Albu-Schäffer, A., Beyer, A., Eiberger, O., Haddadin, S., Stemmer, A., Grunwald, G., et al. (2010). The kuka-dlr lightweight robot arm—a new reference platform for robotics research and manufacturing. In *Robotics (ISR), 2010 41st international symposium on and 2010 6th German conference on robotics (ROBOTIK)*, pages 1–8. VDE.
- [Everts et al., 2009] Everts, M. H., Bekker, H., Roerdink, J. B., and Isenberg, T. (2009). Depth-dependent halos: Illustrative rendering of dense line data. *IEEE Transactions on Visualization and Computer Graphics*, 15(6).
- [Gazis et al., 2014] Gazis, A. N., Beuing, O., Franke, J., Jöllenbeck, B., and Skalej, M. (2014). Bipolar radiofrequency ablation of spinal tumors: predictability, safety and outcome. *The Spine Journal*, 14(4):604–608.
- [Hanses et al., 2016] Hanses, M., Adler, S., and Martin Skalej, S. W., and Elkmann, N. (2016). Robotic Assistance for Spine Interventions. In *15. Jahrestagung der Deutschen Gesellschaft für Computer- und Roboterassistierte Chirurgie (CURAC)*, pages 231–236, Bern, Switzerland.
- [Peterhans et al., 2010] Peterhans, M., Anderegg, S., Gaillard, P., Oliveira-Santos, T., and Weber, S. (2010). A fully automatic calibration framework for navigated ultrasound imaging. In *Engineering in Medicine and Biology Society (EMBC), 2010 Annual International Conference of the IEEE*, pages 1242–1245. IEEE.
- [Ritter et al., 2011] Ritter, F., Boskamp, T., Homeyer, A., Laue, H., Schwier, M., Link, F., and Peitgen, H.-O. (2011). Medical image analysis. *IEEE pulse*, 2(6):60–70.
- [Schaefer et al., 2003] Schaefer, O., Lohrmann, C., Markmiller, M., Uhrmeister, P., and Langer, M. (2003). Combined treatment of a spinal metastasis with radiofrequency heat ablation and vertebroplasty. *American Journal of Roentgenology*, 180(4):1075–1077.
- [Schreiber et al., 2014] Schreiber, J. J., Anderson, P. A., and Hsu, W. K. (2014). Use of computed tomography for assessing bone mineral density. *Neurosurgical focus*, 37(1):E4.
- [Weihsen et al., 2006] Weihsen, A., Ritter, F., Pereira, P. L., Helmberger, T., Hoffmann, R.-T., and Peitgen, H.-O. (2006). Towards a workflow oriented software assistance for the radiofrequency ablation. In *GI Jahrestagung (1)*, pages 507–513.